Mehran University Research Journal of Engineering and Technology

https://doi.org/10.22581/muet1982.2401.2969

2024, 43(1) 165-181

Investigating parametric effects during TIG welding of dissimilar metals

Abdullah *, Shahid Mehmood, Rana Atta ur Rahman

Department of Mechanical Engineering, University of Engineering and Technology, Taxila Pakistan

* Corresponding author: Abdullah, Email: abdullah4@students.uettaxila.edu.pk

Received: 14 November 2023, Accepted: 20 December 2023, Published: 01 January 2024

K E Y W O R D S

TIG Welding

ANOVA

Response Surface Methodology

Ultimate Tensile Strength

Micro-Hardness

A B S T R A C T

This paper explores the optimization of Tungsten-Inert-Gas (TIG) welding process parameters for creating a hybrid structure of Aluminium 6061 and Stainless Steel 304 using a copper filler rod (ER-Cu). The Welding of these two materials has industrial relevance owing to its weight reduction capabilities and environmental benefits. However, Aluminium and Stainless-Steel have different melting points and thermal properties. Aluminium has twice coefficient of thermal expansion and six times coefficient of thermal conductance as compared to Stainless-Steel. This difference often results in residual stresses and brittle intermetallic compounds in the weld region. We have chosen the Welding Current, Welding Speed, and Gas Flow Rate as input parameters, and Ultimate Tensile Strength (UTS) and Micro-hardness as response parameters. We have employed the Response Surface Methodology (RSM) using a Box-Behnken design to evaluate the influence of input parameters on UTS and Micro-hardness. Furthermore, an Analysis of Variance (ANOVA) is conducted to determine the input parameters' significance on the response parameters. Our surface plots demonstrate that UTS improves with increased Welding Current and reduced Welding Speed. Simultaneously, Micro-hardness increases with elevated Welding Speed and decreased current, up to a specific limit. The peak value of UTS (79 MPa) was observed with a Current range of 85-90 A, Speed range of 95-100 mm/min, and Gas Flow Rate of 14.5-15 l/min. On the other hand, maximum Micro-hardness (260HV) was obtained with a Current range of 80-85 A, Speed range of 105-110 mm/min, and Gas Flow Rate of 14.5-15 l/min. This research contributes to improving the manufacturing process of hybrid structures, specifically by optimizing the advantages of both Aluminium and Stainless Steel while addressing the challenges that arise during their combination. The study's conclusions have major consequences for sectors looking to take advantage on the mutually beneficial characteristics of different metals in welding applications.

1. Introduction

The process of welding refers to the fusion of two separate materials using thermal energy, which can originate from a variety of sources including gas combustion, electric arcs, or chemical reactions. A critical process within industrial manufacturing is Gas

Tungsten Arc Welding (GTAW), commonly referred to as Tungsten-Inert-Gas (TIG) welding. This technique is widely employed to join both homogeneous and heterogeneous metal types. TIG welding plant as shown in Fig. 1, utilizes a non-consumable tungsten electrode, with an exceptionally high melting point of 3500°C, to facilitate the creation of the weld.

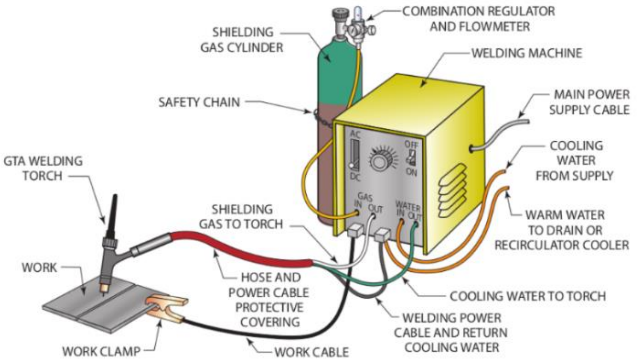

Fig. 1. TIG Welding Plant

The operational mechanism of TIG welding, as shown in Fig. 1, is comparable to that of arc welding. It involves the generation of a high-intensity arc between the electrode and the workpiece, producing heat energy utilized to meld metals together. The need for a filler wire in TIG welding varies based on the workpiece thickness and weld preparation. Typically, the shielding gas choice is dependent on the material to be welded.

TIG welding finds wide applications in sectors such as aerospace and automotive due to its efficacy in welding materials like Stainless Steel, Aluminium and Aluminium alloys, copper-based alloys, and nickel-based alloys. Notably, TIG welding is superior to other arc welding techniques as it produces a robust, durable, corrosion-resistant, and ductile joint. Prior research has explored various welding methods such as friction-welding, friction-stir welding, magnetic-pulse welding, laser-welding, ultrasonic-spot welding, explosive-welding, TIG-MIG hybrid welding, and TIG welding for the fusion of Aluminium and Stainless Steel. This study adopts TIG welding for the fusion of these metals because of its potential to create robust, clean, durable welds, and its cost-effectiveness.

The welding process can generally be classified into fusion welding and pressure welding, the different types of welding are shown in Fig. 2.

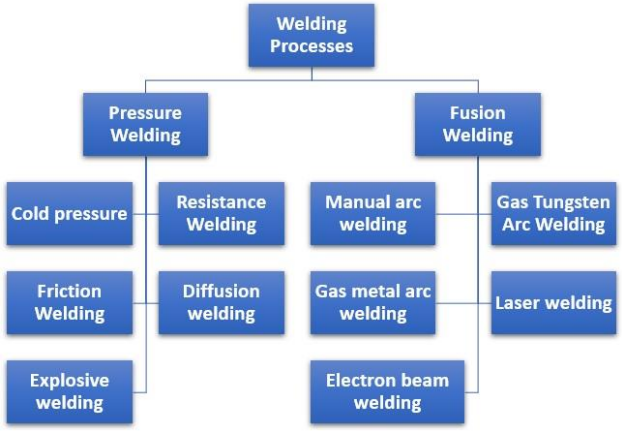

Fig. 2. Classification of Welding Processes

1.1 Effect of GTAW Parameters on Tensile Strength

Previous studies have examined various aspects of welding processes between different metal types. For instance, a study by Cheepu et al analyzed dissimilar welding between 304 Stainless Steel and 5083 Aluminium using the Gas-Tungsten-Arc welding brazing method with an Al-Cu eutectic filler-metal [1]. They scrutinized the influence of this filler on tensile strength across a current range of 95 A to 180 A, discovering that an optimum tensile strength of 95 MPa was reached at a current of 140 A.

In another study, He et al explored the implications of the hot twin wire technique on welding Aluminium and stainless-steel joints via TIG welding brazing [2]. Their findings indicated that this technique enabled a lower Welding Current range of 83 A to 120 A compared to the typical 100 A to 120 A necessary for a stable welding process. As the Welding Current was increased from 83 A to 115 A, they noticed a decrease in joint strength from 280 MPa to 171 MPa.

Kotari et al. employed a BCuP-4 copper filler wire for the fusion of Aluminium 6061 and Stainless Steel 304 [3]. Utilizing the Taguchi method, they varied several welding parameters: currents between 90-140 A, speeds from 100-120 mm/min, and gas flows between 8-10 l/min. Their findings revealed that optimal tensile strength, reaching up to 132 MPa, was achieved with a Welding Current of 100 A, speed of 90 mm/min, and a Gas Flow Rate of 9 l/min.

Singh et al. employed the Taguchi approach to investigate the influence of various welding parameters on the tensile strength of the 5083 Aluminium alloy [4]. Specifically, they altered Welding Speeds in the range of 89-102 mm/min, currents from 210-240 A, and Gas Flow Rates from 6-7 l/min. They determined that the apex tensile strength, reaching 129 MPa, was achieved under conditions of 240 A Welding Current, a 7 l/min

Gas Flow Rate, and a Welding Speed of 98 mm/min. Additionally, they noted a pattern: with a static current, an initial rise in Welding Speed led to an enhancement in joint strength. However, upon further escalation in speed, the strength of the joint showed a decline.

In an investigation performed by J.Pasupathy [5], the influence of TIG welding variables, including Welding Current and velocity, on the bonding strength between low carbon steel and AA1050 was scrutinized. Leveraging the Taguchi technique, he delineated the paramount settings to attain peak strength. A subsequent validation experiment was executed to corroborate the validity of the Taguchi approach. The study revealed that an apex strength of 61.37 MPa was realized at a Welding Current setting of 135A coupled with a progression speed of 3.2 mm/sec.

Lastly, a study by Ishak et al investigated the TIG welding process on Aluminium 6061, focusing on the impact of filler and current on tensile strength, Micro-hardness, and microstructure [6]. They found that using the filler ER5356 resulted in the highest tensile strength of 171.53 MPa compared to fillers ER4043 and ER4047, with tensile strengths of 167.34 MPa and 168.03 MPa, respectively. Moreover, a Welding Current of 60 A yielded a higher tensile strength than 70 A.

L. H. Shah investigate the effects of welding voltage and filler-metals on weld joint of Aluminium 6061 and Stainless Steel 304. The research found that using ER5356 filler for welding led to an increase in Si particles, enhancing the metal's strength and joint characteristics. On the other hand, ER308LSi filler welding led to the formation of chromium carbide, increasing Micro-hardness but also the brittleness. The highest tensile strength recorded was 104.4MPa with ER5356, while ER308LSi yielded a top strength of 61.76MPa [18].

1.2 Effect of GTAW Parameters on Micro-hardness

Ishak et al. explored the role of filler material and current in influencing the Micro-hardness, tensile strength, and microstructure during the TIG welding of Aluminium 6061 [6]. Their results indicated that employing the ER5356 filler yielded a Micro-hardness value of 72.9 HV, which was notably higher than the 59.3 HV and 57.6 HV obtained when using ER4043 and ER4047, respectively. Additionally, the research underscored that an upsurge in the Welding Current correspondingly augmented the Micro-hardness.

Chuaiphan undertook an optimization study on TIG welding parameters for the joint welding of AISI 205 and AISI 216, employing the ER307 filler [7]. The investigation encompassed Welding Speeds from 1 to 3.5 mm/s and variations in hydrogen content within argon gas, ranging from 1% to 6%. Parameters under evaluation included microstructure, mechanical attributes, and resistance to pitting corrosion. It was discerned that a speed of 3.5 mm/s led to superior Micro-hardness values as opposed to those achieved at 2.5 mm/s or 1 mm/s. This elevated Micro-hardness at higher speeds could be attributed to the refining of the grain structure within the welding zone. Moreover, the delta ferrite content also experienced an uptick at this speed, which in turn, contributed to the enhanced Ultimate Tensile Strength (UTS) of the welded joint.

Anteneh Teferi Assefa, alongside his team, embarked on an exploration concerning the influence of TIG welding parameters on the microstructure and mechanical attributes of low carbon steel varieties SS 316 and AISI 1020 [8]. Their study enveloped a multitude of process determinants, including Welding Current, gas flow dynamics, and the choice of filler metal. Outcomes such as tensile strength, Micro-hardness, and flexural resilience were meticulously examined. For their experimental configuration, they implemented an L16 orthogonal array. Their investigations elucidated that the optimal Micro-hardness was achieved under conditions of a 130 A Welding Current, a 2 mm root gap, and a 16 l/min Gas Flow Rate. Furthermore, a discernible trend was observed where Micro-hardness exhibited an amplification in tandem with increments in both Welding Current and Gas Flow Rate.

In another research, Mohamed Farid Benlamnouar and his team utilized the Taguchi approach to fine-tune the TIG welding parameters when amalgamating austenitic Stainless Steel 304L with low alloy steel X70 [15]. Parameters under investigation included Welding Current, welding velocity, and the Gas Flow Rate. Key response metrics were tensile strength and Micro-hardness, with experiments structured around the L9 orthogonal array. Their findings underscored the paramount influence of the Gas Flow Rate, notably enhancing the tensile strength while simultaneously mitigating the Micro-hardness of the welded joints. The research pinpointed an optimal set of parameters: a welding velocity of 70 m/min, a current intensity of 70 A, and a Gas Flow Rate set at 8 l/min.

Reddy explored the optimization of Micro-hardness in SS 304L and SS 430 TIG welding joints using response surface methodology [9]. The experimental design matrix was developed using the Box Behnken

design with five central points. The process parameters under consideration included Welding Current (ranging from 120 to 180), wire feed (from 0.62 to 0.82 mm/min) and traveling speed (from 0.070 to 0.080 mm/min). The study's findings suggested that Micro-hardness improved with increasing current and Welding Speed. The peak Micro-hardness value of 231.079 HV was observed at 120 A, a Wire-Feed of 0.82 mm/min, and a traveling speed of 0.0779 mm/min.

Vishal Chaudhari optimizes the tig welding parameters for dissimilar welding of stainless-steel and mild steel. Maximum Micro-hardness was noted at 150 amps, 22 volts, and a Gas Flow Rate of 12liters per minute [19].

Navaneeswar Reddy optimize the Micro-hardness of SS 304 and SS 430 weld joint. The highest Micro-hardness, at 231.079 HV, was noted with a Welding Current of 120 A, Wire-Feed-Rate of 0.82 mm/min, and travel speed of 0.0779 mm/min [9].

1.3 Effect of GTAW Parameters on Microstructure

Nguyen Van Nhat embarked on a study examining the TIG welding process, which involved dissimilar welding of Aluminium and steel using ER 4047 Al Si filler [10]. The study highlighted the formation of a thin, homogeneous intermetallic layer that was 2 micro-meters in thickness, along the welding joint. This outcome was linked to the Silicon atoms in the filler-metal inhibiting the diffusion of Fe atoms into the molten state of Aluminium. Furthermore, the study noted a reduction in the heat-affected zone's size.

In another research, Huan He investigated the influence of nocolok flux and nickel powder on the TIG welding brazing process of Aluminium and steel [11]. The addition of nickel powder into the flux was found to substantially reduce the formation of intermetallic compounds, while concurrently transforming the phase from $FeAl_6$ to Al_9FeNi. This, in turn, boosted the tensile properties of the joint.

In a study involving Aluminium 6061, M. Ishak et al studied the implications of fillers and current on the microstructure, tensile strength, and Micro-hardness in the TIG welding process [6]. The researchers observed that the use of ER5356 filler and a Welding Current of 70 A resulted in welds with smaller grain structures, while the usage of ER4043 and ER4047 fillers led to larger grain structures.

Shuhai Chen investigated laser welding of steel and Aluminium, comparing the outcomes of joints with and without nickel foil [12]. The absence of nickel foil led to the formation of brittle FeAl / $FeAl_3$ intermetallic structures at the interface. In contrast, the incorporation of nickel foil resulted in a Ni1Al / $FeAl_3$ structure that effectively prevented cracking.

In J.L. Song's study, the intermetallic layer of Tungsten inert gas weld brazing joints between Aluminium and steel was analyzed using 4047 Al-12Si and 2319 Al-6Cu filler metals [13]. The TIG heat arc was applied to warm the base and filler metals, with the joint being formed through the interaction of liquid Aluminium with solid steel. The Al-12Si filler-metal joint comprised two brittle intermetallic layers, $5Al_8Fe_2Si$ in the weld seam and $(AlSi)_{13}Fe_4$ on the steel side. On the other hand, the Al-6Cu filler metal joint had a crack-resistant layer and demonstrated a tensile-strength of 155 MPa, whereas the Al-12Si filler metal joint showed a tensile strength of 100 MPa.

Gilang Sigit Saputro investigated the impact of Micro-hardness and microstructure on the weld joints of galvanized steel and Aluminium, using Al-Si-4043 filler metal in TIG welding and varying the current and Gas Flow Rate [14]. The study found that the thickness of the intermetallic layer increased with a rise in Welding Current up to 80 A, while an increment in the Gas Flow Rate resulted in a decrease in the layer's thickness.

1.4 Effect of Interlayer/Filler on Mechanical Properties

J.L. Song spearheaded a research project exploring the impact of Silicon addition in the filler-metal on the welds between Aluminium and steel [13]. The study made use of three distinct types of filler-metals, namely pure Al, AlSi5, and AlSi12. The results underscored that Si addition mitigated the thickness of the IMC layer and hindered its accumulation. The highest strength of 125.2 MPa was observed with the use of AlSi5 filler metal.

Chen Shuhai undertook a detailed study on the laser welding of Aluminium and steel lap joints using a nickel interlayer [12]. This study demonstrated that the introduction of a nickel foil not only enhanced the tensile strength but also reduced the joint's Micro-hardness. Importantly, the presence of the foil prevented the formation of cracks by facilitating the creation of $NiAl_3$ at the weld interface.

In a separate study, Xue-long CAO assessed the characteristics of the laser welding joint between the 6061 Aluminium alloy and 304 stainless-steel. This involved the use of varied laser parameters and Copper Nickel interlayers [17]. It was determined that fine-tuning the thickness of the Cu interlayer to 0.02 mm led

to a significant increase in the shear force, which rose to 1350.96 N.

Lastly, Muralimohann scrutinized the TIG welding brazing process of Stainless Steel and Aluminium alloy using an Al-Cu filler [1]. The experiment yielded a maximum tensile strength of 95 MPa and a peak Micro-hardness of 600 HV.

Tianyu Xu investigated the effect of nickel foil thickness on laser welding of Aluminium and steel lap joint. Using a nickel foil of 20µm thickness can extend the penetration depth to 382µm and enhance shear resistance to 103N/mm, marking a 92% rise compared to joints devoid of the nickel foil [17].

Pratishtha Sharma compare the activated-flux-GTAW and Multi pass GTAW in P92 steel and 304H steel dissimilar welding. The average distortion observed for P92 steel and 304H ASS using Activated-Flux-GTAW was 0.70° and 0.98°, respectively. However, when utilizing multi-pass welding, the distortion increased to 2.34° and 3.21° for P92 steel and 304H ASS, respectively. The higher distortion can be linked to the cyclical heating and cooling during welding [20].

P. Kannan examine the effect of silver interlayer in the friction-welding of 6061 T6 Aluminium alloy and AISI 304 stainless-steel. The implementation of a silver interlayer in the welding process leads to a 3.15% reduction in fracture particles compared to processes without an interlayer, while improving tensile strength. It also causes softening in the welded area, inducing a spread of residual stress from the weld seam. [16]

It is true that the individual effects of welding parameters (current, speed, and gas flow rate) on materials such as AL-6061 and SS-304 have been reported in the literature, our research presents a novel and unprecedented combination of factors. Specifically, our study focuses on the TIG welding of Aluminium 6061 and Stainless Steel 304 using a copper (Cu) filler rod—a unique alloy combination not extensively explored in existing literature.

To the best of my knowledge, no prior work has been conducted or published on the TIG welding of Aluminium 6061 and Stainless Steel 304 with the use of a copper filler rod. Additionally, the specific parameter ranges we investigated, including a current range of 80 to 100A, welding speed range of 90 to 110 mm/min, and gas flow rate of 13 to 15 l/min, represent a novel contribution to the field. These specific parameter combinations and the use of copper as a filler material contribute to the originality of our work.

In essence, our research not only fills a significant gap by exploring an uncharted territory in dissimilar metal welding but also introduces a unique set of welding parameters, providing valuable insights that were previously absent in the existing body of literature. The combination of dissimilar materials, the use of a specific filler material, and the exploration of distinct parameter ranges collectively constitute the distinctive contribution of our work to the field of TIG welding of dissimilar metals.

2. Methodology

Fig. 3 illustrates the research approach used in this study.

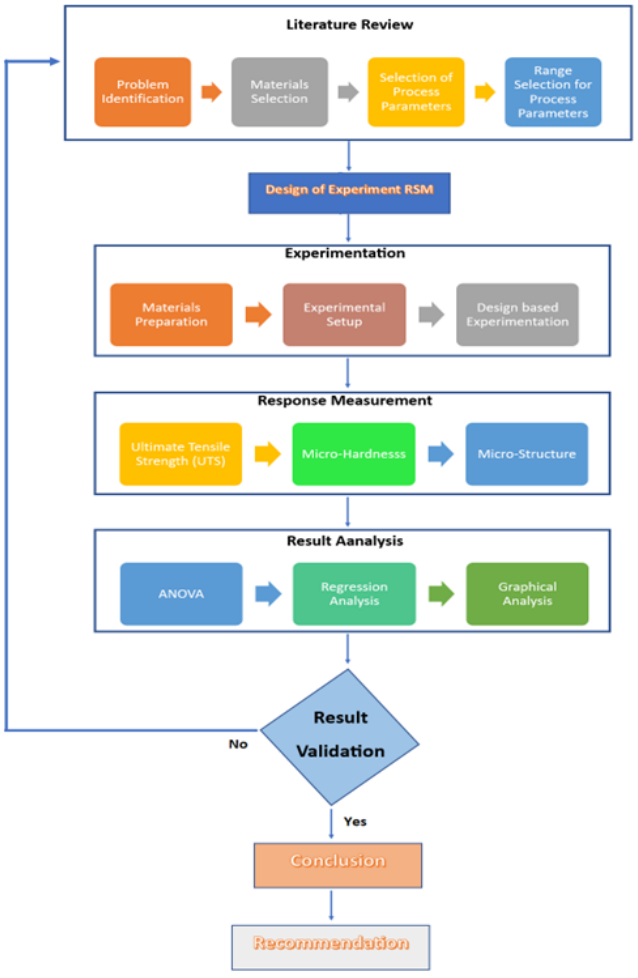

Fig. 3. Research Methodology

Table 1 provides a list of the chemical compositions of the base and filler metals.

Table 1

Chemical composition (weight %) of selected materials

Elements	Aluminium-6061	Stainless-Steel	ER-Cu filler rod
Al	Bal.		0.02
Fe	0.70	Bal.	0.40
Cu	0.40	0.009	Bal.
Cr	0.35	18.08	Trace
C		0.048	
Mg	1.20		
Mn	0.15	1.228	0.65
Si	0.80	0.419	0.58
Ti	0.15		0.28
Zn	0.25		0.01
P		0.031	0.003
S		0.002	0.03
Mo		0.011	
Ni		8.113	0.02
Pb			0.02
Sn			0.01
Co			0.03

The following parameters are considered during the TIG Welding process.

1. Welding Current
2. Welding Speed
3. Gas Flow Rate

The WSE-400 AC/DC/MIX TIG is a welding machine as shown in Fig. 4, is designed for Tungsten Inert Gas (TIG) welding. It can produce both Alternating-Current (AC) and Direct-Current (DC) power, as well as a combination of both, making it suitable for welding a variety of metals, including Aluminium, steel, copper, and other alloys.

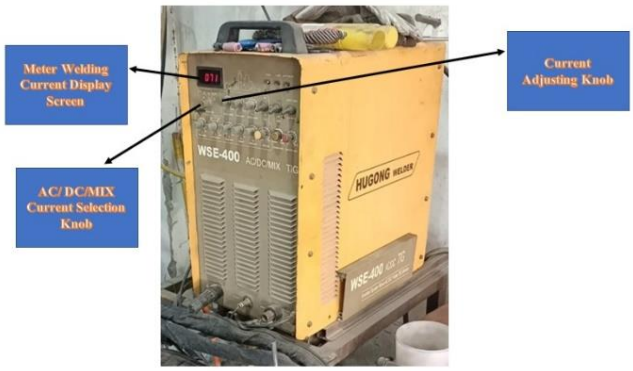

Fig. 4. WSE-400 AC/DC/MIX TIG Welding Machine

Table 2 outlines the process parameters and their corresponding levels.

Table 2

Process Parameters and their Levels

Process Parameters	Level 1	Level 2
Welding Current (A)	80	100
Welding Speed (mm/min)	90	110
Gas Flow Rate (l/min)	13	15

Table 3 displays the experimental conditions for the conducted experiments.

Table 3

Experimental settings

Sr. No.	Parameters	Values
1	Welding Current	80-100A
2	Welding Speed	90-110 mm/min
3	Gas Flow Rate	13-15 l/min
4	Filler rode material	ER-Cu rod
5	Filler rode	2.4mm diameter
6	Electrode material	Tungsten
7	Polarity	AC pulse
8	Type of groove	V type
9	Shielding gas	Argon gas

Table 4 displays the experimental design matrix used for this research. For this study, Aluminium 6061 and Stainless Steel 304 plates, each 3mm thick, were utilized as substrates. ER-Cu, a 2.4 mm diameter copper rod, was the chosen filler. The plates, sized 60 mm x 55 mm, were prepared using a Hand Grinder and given a V groove by incising a 45° angle. The plates were polished with a sandpaper and clean with acetone before being fixed into place. Fig. 5 visually represents the materials preparation process. Finally, the clamped plates were placed on the welding workstation.

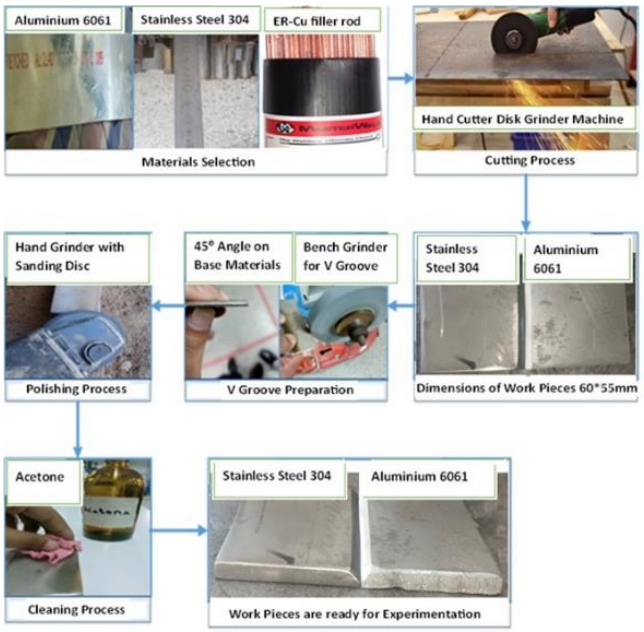

Fig. 5. Materials preparation process

The welding specimens of the experiments conducted after the preparation of the materials is shown in Fig. 6.

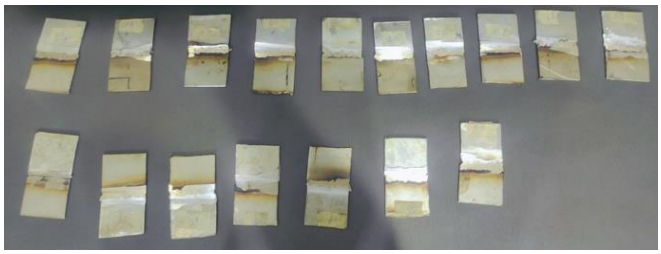

Fig. 6. Welded Specimens

The surface Grinding machine as shown in Fig. 7, is used to smooth the welding area of specimens as shown in Fig. 8.

Fig. 7. Surface Grinding Machine

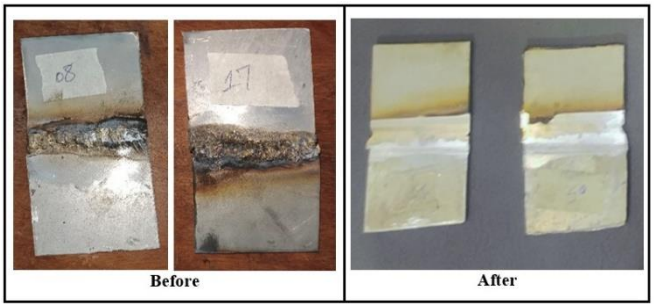

Fig. 8. Before and After the use of Surface Grinding Machine

Tensile samples were prepared by cutting them perpendicular to the weld line using a wire EDM. The process of preparing tensile samples is shown in Fig. 9.

Fig. 9. Wire Cut EDM Machine for Tensile Samples preparation

The ASTM E8/E8m-15a standard was followed to carry out a tensile test [21]. Fig. 10 illustrates the standard sample used for the test. The sample was prepared using wire EDM cutting technique perpendicular to the weld line.

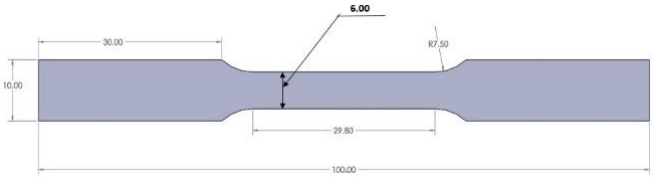

Fig. 10. Tensile standard specimen

Based on ASTM E8/E8m-15a, a total of seventeen samples were prepared as shown in Fig. 11.

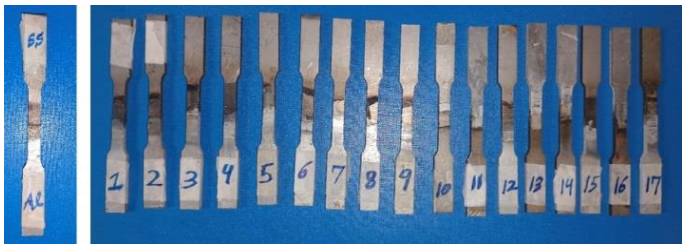

Fig. 11. Tensile samples

The tests were performed using an Gaotiejian Instrument UTM machine as shown in Fig. 12, with a 10KN to 1000KN capacity, and a strain rate of 1mm/min was applied.

Fig. 12. UTM Apparatus

The Micro-Vickers-Hardness-Tester was utilized to measure the Micro-hardness of the welding area. The procedure, which followed the standard protocol [22], involved a load of 1kgf and a load duration of 10 seconds. The equipment used for this purpose is shown in Fig. 13, which portrays the tests conducted on the chosen region.

Fig. 13. Vickers Micro-hardness Tester

The fracture area microstructure of the tensile specimens was imaged using a Scanning Electron Microscope (SEM). Photos were shot at 20 µm on each fractured side. Fig. 14 shows the image of SEM.

Fig. 14. Scanning-Electron-Microscope (SEM)

3. Results and Discussion

After testing, the samples were fractured, and their images are presented in Fig. 15.

Fig. 15. Fractured tensile specimens

The processing parameters and corresponding UTS and Micro-hardness values of the Al and SS TIG weld joint are presented in Table 4.

Table 4

Ultimate Tensile Strength (UTS) and Micro-hardness Results

Run	Welding Current (A)	Welding Speed mm/min	Gas Flow Rate l/min	Ultimate Tensile Strength (UTS)	Micro-hardness (HV)
1	100	100	13	29	195
2	100	90	14	27	95
3	90	100	14	68.78	172
4	90	90	13	16	104
5	90	90	15	69	239
6	80	110	14	26.34	231
7	80	90	14	36	148
8	90	110	13	20	255
9	90	100	14	66.2	162
10	80	100	15	79	262
11	100	110	14	15.11	164
12	90	110	15	43	196
13	90	100	14	71	155
14	90	100	14	76.98	169
15	90	100	14	69	178
16	100	100	15	23.46	238
17	80	100	13	14	256

The Fig. 16 displays the residuals plot for UTS. The plot indicates that there are only a few data points that deviate significantly from the trend line, suggesting that the error distribution is normal.

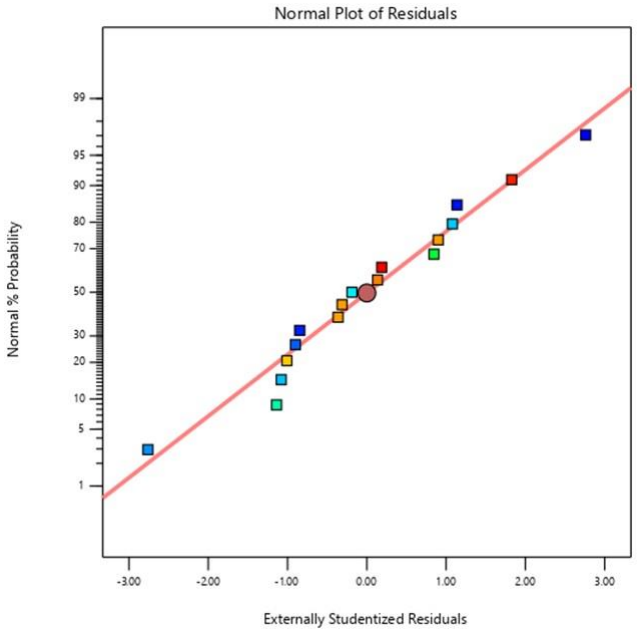

Fig. 16: Normal plot of residual for UTS

The adequacy of the model was confirmed by plotting the actual values of UTS against the predicted values, as shown in Fig. 17. The points representing the actual and predicted values are closely clustered, indicating a good fit between the model and the data.

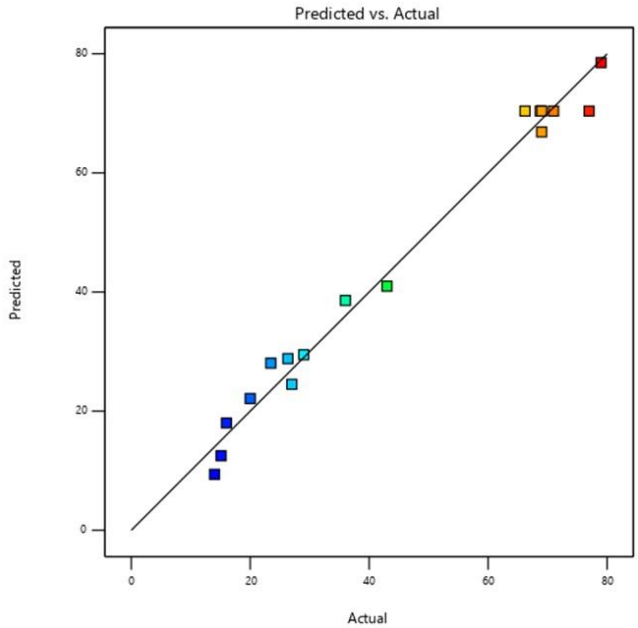

Fig. 17: Predicted vs. Actual UTS values

Fig. 18 presents a 3D surface graph showing how Welding Current and speed impact the weld joint's maximum tensile strength. The graph suggests an improvement in joint strength with higher current and slower speed. Initially, an increase in speed boosts tensile strength, but too much speed leads to insufficient heat in the weld pool, causing incomplete penetration and a drop in tensile strength [3, 23].

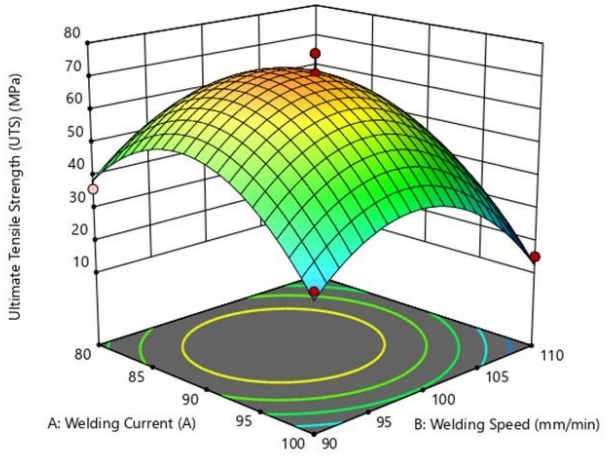

Fig. 18. Surface plot of Welding Current and Welding Speed for UTS

The Fig. 19 reveals that a rise in Welding Current and gas flow improves the Ultimate Tensile Strength (UTS) of the joint. This happens as more heat from higher current melts the base metal, and increased gas flow protects it, creating a stronger joint. However, excessive current could over-penetrate the Aluminium, which might reduce the UTS of the joint. [5, 8].

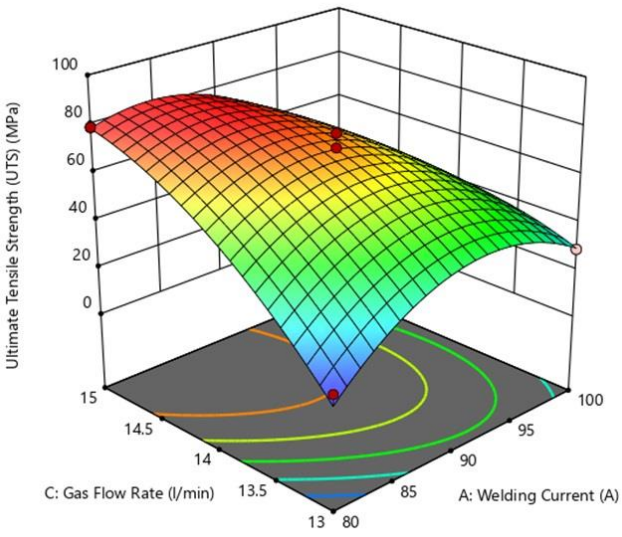

Fig. 19. Surface plot of Welding Current and Gas Flow Rate for UTS

Fig. 20 demonstrates a correlation between the Gas Flow Rate and Welding Speed, and the Ultimate Tensile Strength (UTS). Greater Gas Flow Rates improve environmental shielding, and faster Welding Speeds help avoid excess heat. Nevertheless, an overly rapid Welding Speed may lower joint strength by diminishing weld penetration and root weld metal, a finding that aligns with Wichan Chuaiphan's optimization research on Aluminium and steel [23].

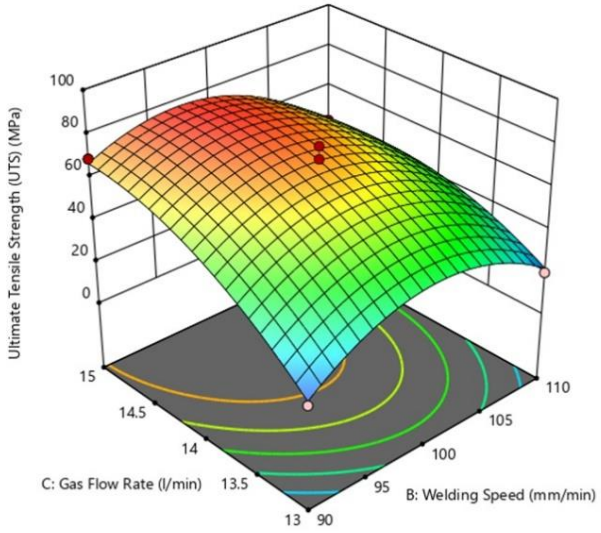

Fig. 20. Surface plot of Welding Speed and Gas Flow Rate for UTS

Fig. 21 presents a normal probability plot for the Micro-hardness residuals in the Al-SS weld joint. The proximity of all points to the line suggests a normal distribution of the error.

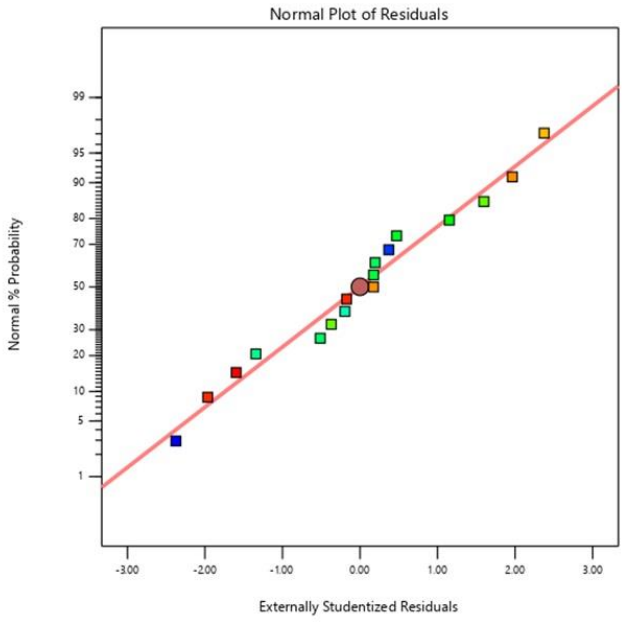

Fig. 21. Normal plot of residual for Micro-hardness

Fig. 22 illustrates a comparison between forecasted and real Micro-hardness values of the Al-SS weld joint at the interface. The proximity of points to the prediction line signifies high correlation between actual and anticipated data, corroborating the model's effectiveness.

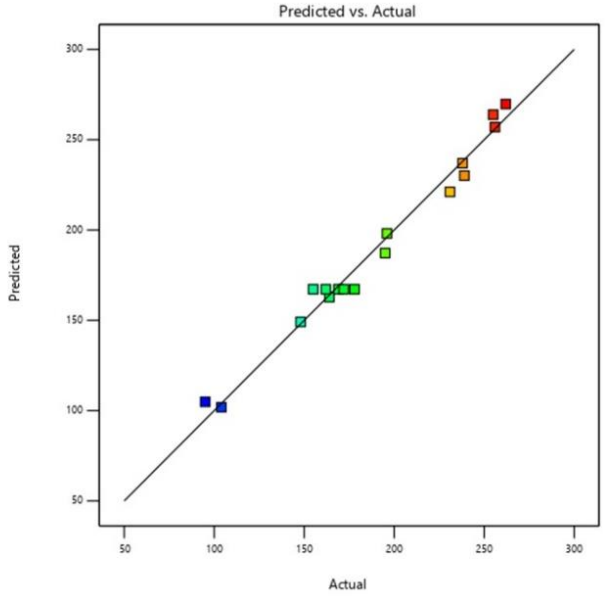

Fig. 22. Predicted vs. Actual Micro-hardness values

Fig. 23 presents a 3D surface plot illustrating that greater Micro-hardness levels can be achieved with faster Welding Speeds and lower Welding Currents. This is because increased Welding Speed results in rapid cooling, producing a finer grain structure and thus enhancing the Micro-hardness of the weld joint [8, 24].

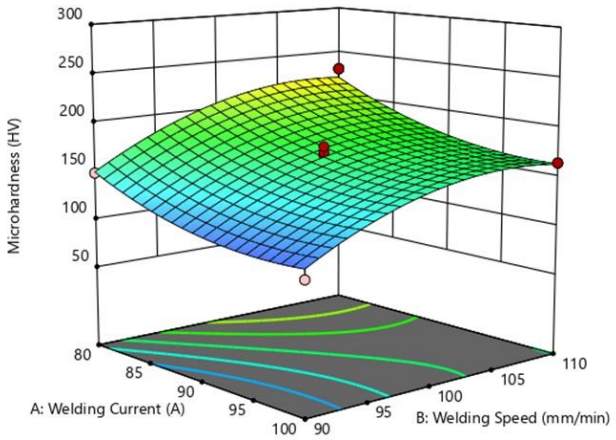

Fig. 23. Surface plot of Welding Current and Welding Speed for Micro-hardness

Fig. 24 indicates that augmenting the gas flow and reducing the Welding Current raises the Micro-hardness. While an initial upturn in gas flow reduces Micro-hardness, continued escalation enhances the weld pool's shielding, thus boosting Micro-hardness levels [8, 25].

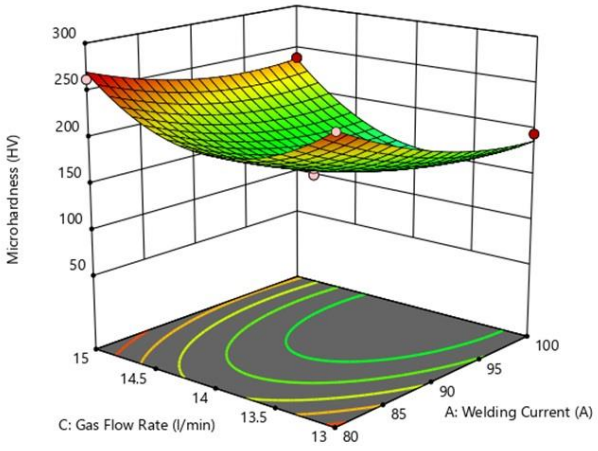

Fig. 24. Surface plot of Welding Current and Gas Flow Rate for Micro-hardness

Fig. 25 indicates that Micro-hardness escalates with higher Welding Speed and Gas Flow Rate. Faster cooling due to increased Welding Speed generates finer grain structures, improving Micro-hardness. Further, superior shielding from greater gas flow also enhances Micro-hardness. This aligns with previous studies' findings [23, 24].

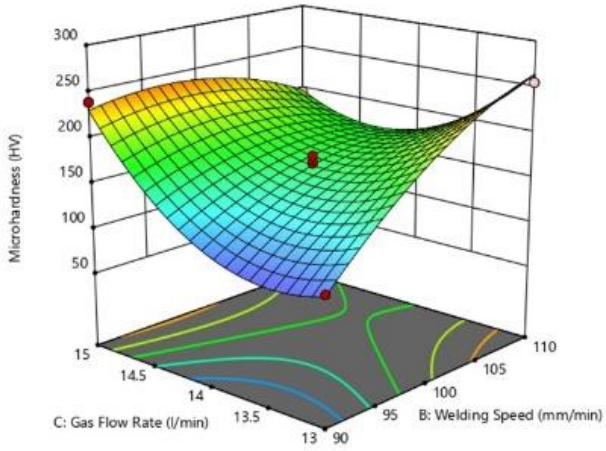

Fig. 25. Surface plot of Welding Speed and Gas Flow Rate for Micro-hardness

3.1 Validation of Results

The validity of both the UTS model and Micro-hardness model was tested through three confirmatory tests.

$$\text{Percentage Error} = \frac{|Experimental\ Value - Predicted\ Value|}{Predicted\ Value}$$

3.1.1 For Ultimate Tensile Strength (UTS)

Table 5 shows the observed and estimated Ultimate Tensile Strength (UTS) values, including the percent errors, from the experiment. The data implies a significant alignment between these observed and projected strengths.

Table 5

Confirmation test result for UTS

Exp. No.	Welding Current (A)	Welding Speed mm/min	Gas Flow Rate l/min	Exp. Value	Predicted	% Error
1	90	100	14	66.2	63.16	4.81
2	100	100	13	29	26.94	7.64
3	80	110	14	26	25.12	3.50

3.1.2 For micro-hardness

Table 6 shows both measured and estimated Micro-hardness Fig.s at the weld area of the connection, alongside related percentage inaccuracies. The data suggest a fair association between observed and forecasted Micro-hardness values.

Table 6

Confirmation test result for Micro-hardness

Exp. No.	Welding Current (A)	Welding Speed mm/min	Gas Flow Rate l/min	Exp. Value	Predicted	% Error
1	90	100	14	161	153.2	5.09
2	100	100	13	195	189.2	3.06
3	80	110	14	230	221.4	3.89

3.2 Optimization and Contour Plots

3.2.1 For Ultimate Tensile Strength (UTS)

Fig. 26 displays a contour map, representing the optimization of Ultimate Tensile Strength (UTS) using Welding Speed and current. It suggests an optimal UTS of 71MPa at a current between 85-90A and speed within 95-100 mm/min.

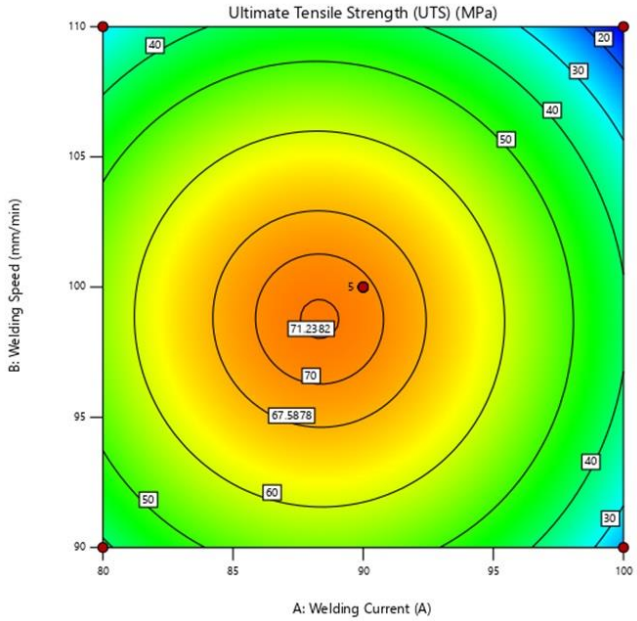

Fig. 26. Contour plot of Welding Current and Welding Speed for UTS

Fig. 27 presents the relationship between Welding Current and Gas Flow Rate through a contour plot, showing that a UTS of 79 MPa is achievable with a current of 85-90 A and Gas Flow Rate of 14.5-15 l/min. Lastly, Fig. 4.15 illustrates the contour plot showing how Welding Speed and Gas Flow Rate contribute to the optimal Micro-hardness and Ultimate Tensile Strength (UTS).

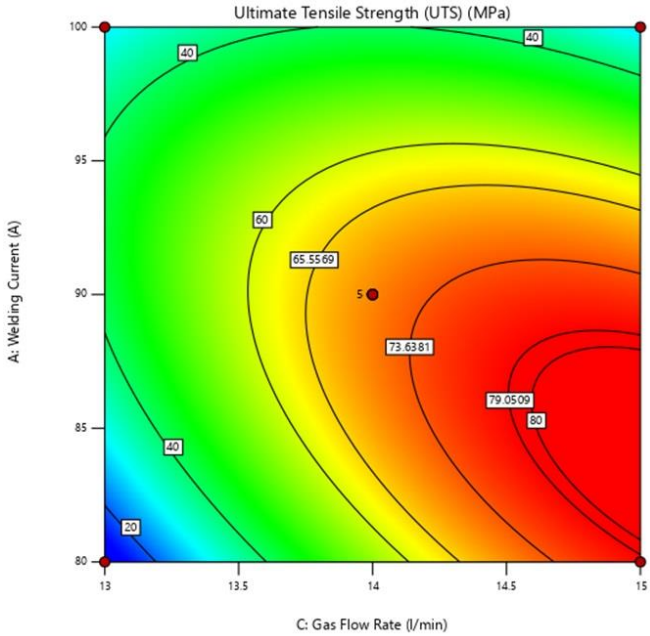

Fig. 27. Contour plot of Welding Current and Gas Flow Rate for UTS

Fig. 28 demonstrates that the peak UTS value of 77 MPa is achieved with a Gas Flow Rate of 14.5-15 l/min and a Welding Speed of 95-100 mm/min.

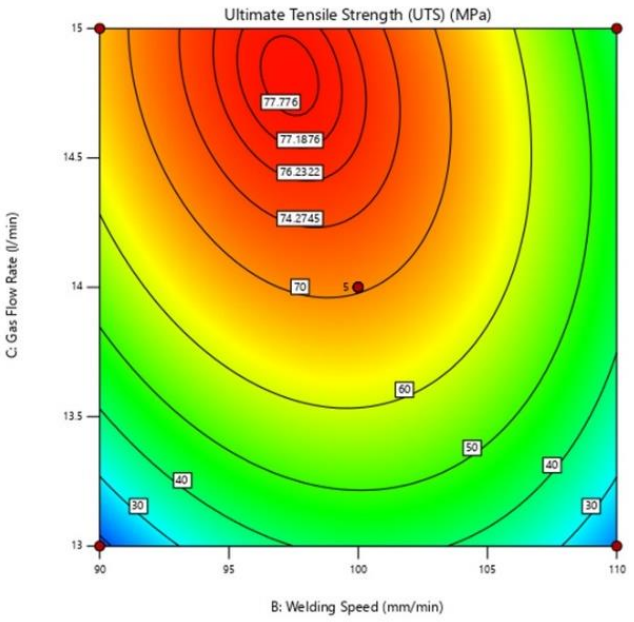

Fig. 28. Contour plot of Welding Speed and Gas Flow Rate for UTS

3.2.2 For micro-hardness

Fig. 29 displays a contour map, demonstrating the joint impact of Welding Speed and current on Micro-hardness. It highlights that optimal Micro-hardness, 216 HV, is attained at a Welding Speed of 105-110 mm/min and current of 80-85 A.

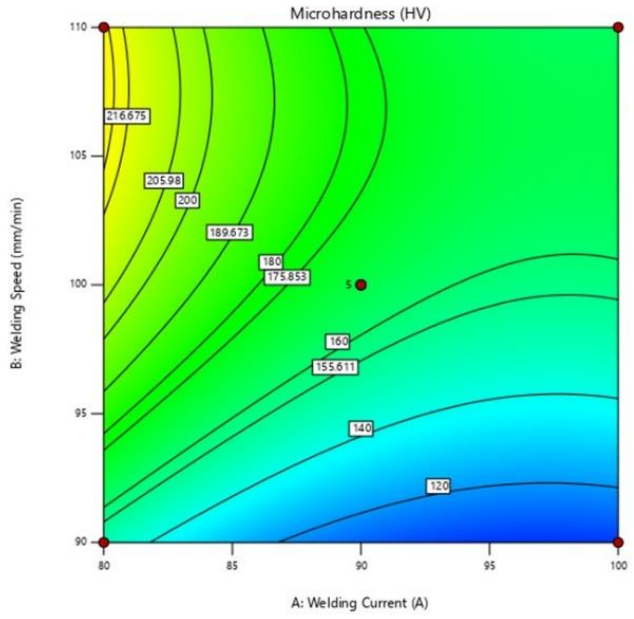

Fig. 29. Contour plot of Welding Current and Welding Speed for Micro-hardness

The contour plot depicted in Fig. 30 shows that the concurrent influence of Welding Current and gas-flow rate on the Al-SS weld joint's Micro-hardness. The data reveals the peak Micro-hardness of 260 HV is obtained with 80-85 A Welding Current and 14.5-15 l/min gas-flow rate.

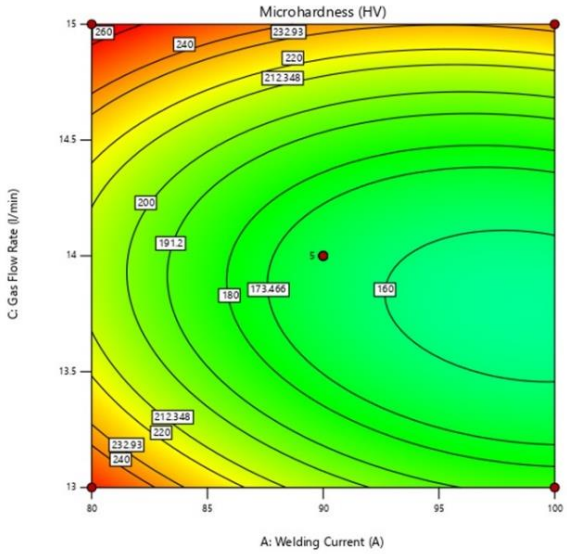

Fig. 30. Contour plot of Welding Current and gas-flow rate for Micro-hardness

Fig. 31 illustrates the optimization contour plot for Micro-hardness using Welding Speed and gas-flow rate. It reveals that maximum Micro-hardness of 250 HV is achievable with a Welding Speed of 105-110 mm/min and gas flow of 13-13.5 l/min.

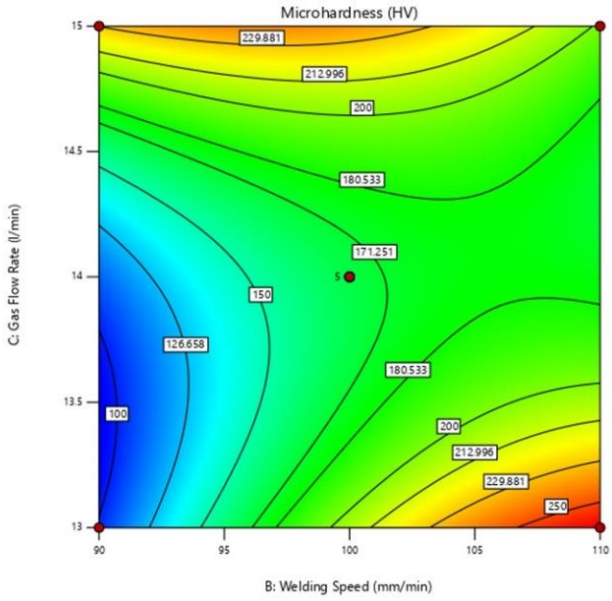

Fig. 31. Contour plot of Welding Speed and Gas Flow Rate for Micro-hardness

3.3 Scanning Electron Microscope (SEM) Results

The study utilized a scanning electron microscope to investigate the fracture patterns in Aluminium and steel weld joints. Both high and low Ultimate Tensile Strength (UTS) joint fractures were studied. Dimpled fracture surface, indicative of weld joint ductility, was observed in a sample with a tensile strength of 79 MPa (as shown in Fig. 32. Full engagement of filler metal with base metals was achieved at parameters of 80 A current, 100 mm/min speed, and 15 l/min Gas Flow Rate. This led to high tensile strength and fracture within the weld zone, aligning with findings from Research [26].

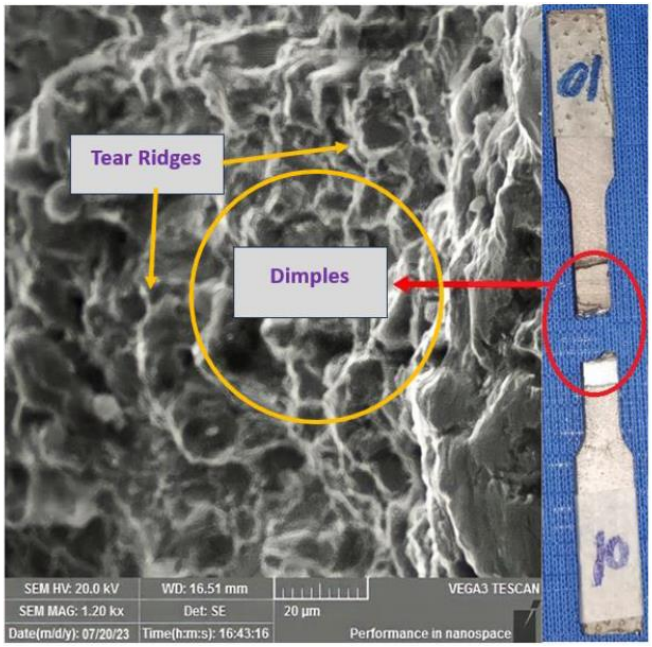

Fig. 32. Fractography of sample 10 (High Strength)

The bonding of the filler metal is ineffective, causing a drop in interface temperatures when welding at 80 A, 100 mm/min, and a Gas Flow Rate of 13 l/min. This leads to brittle breakages on the Stainless-Steel part of the joint. A sample showing a tensile strength of 14MPa presents brittle fracture along with voids and cracks, as shown in Fig. 33.

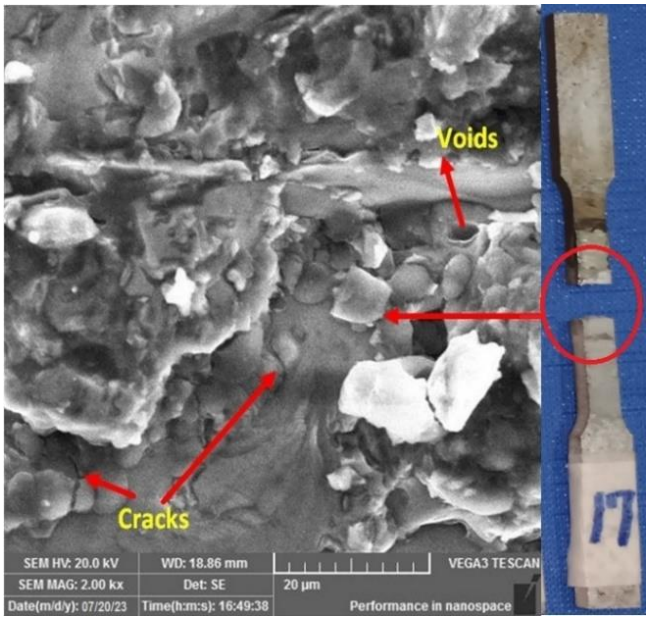

Fig. 33. Fractography of sample 17 (Low strength)

Fig. 34 shows the Stress Strain Curve for High Tensie Strength joint and Fig. 35 shows the Stress Strain Curve for Low Tensie Strength joint.

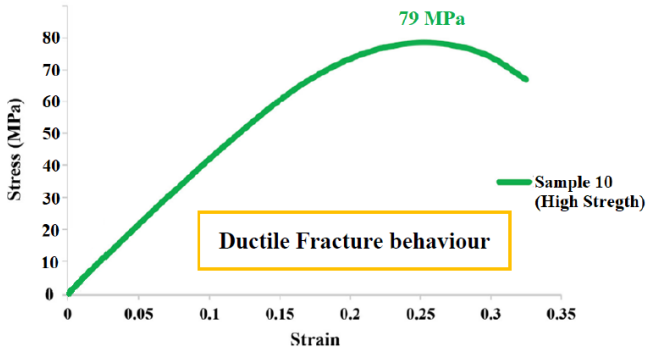

Fig. 34. Stress vs Strain Curve for High Tensile Strength

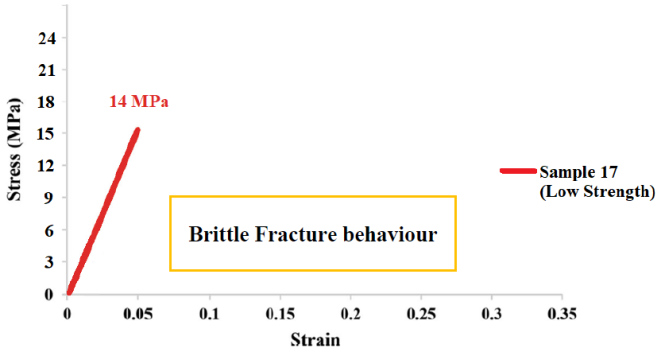

Fig. 35. Stress vs Strain Curve for Low Tensile Strength

4. Conclusion

This research aimed to create a weld joint between Aluminium 6061 and Stainless Steel 304 via TIG welding, using an ER-Cu filler rod. The focus was on examining how welding parameters like current, speed, and Gas Flow Rate influenced the mechanical attributes of the welded joint.

High Tensile Strength of 79MPa and Maximum value of Micro-hardness 262HV was achieved at a Welding Current of 80A, Welding Speed of 100mm/min and Gas flow rate of 15l/min.

Similarly, Low Tensile Strength of 14MPa was obtained at a Welding Current of 80A, Welding Speed of 100mm/min and Gas flow rate of 13l/min. And Minimum value of Micro-hardness 95HV was obtained at a Welding Current of 100A, Welding Speed of 90mm/min and Gas flow rate of 14l/min. Response surface and contour plots were leveraged to analyze the impact on tensile strength and hardness, resulting in mathematical models for prediction. To confirm these findings, tests were performed.

- Key conclusions include the successful welding of robust TIG welds using a copper ER-Cu filler rod.
- According to ANOVA analysis, Welding Current significantly influenced tensile strength (Welding Current 78%, Welding Speed 14.9% and Gas flow rate 7.1%), whereas Welding Speed affected Micro-hardness most (Welding Current 33%, Welding Speed 54% and Gas flow rate 12.13%).
- The surface plots showed a rise in tensile strength with an increase in Welding Current and speed, up to a limit, and a similar trend was noted for Micro-hardness with increased speed and Gas Flow Rate.
- The contour plots illustrated that an optimal UTS of 79MPa was achieved at a current setting between 85-90 A, the Welding Speed of 95-100 mm/min and a Gas Flow Rate of 14.5-15 l/min. The maximum Micro-hardness of 260HV was reached at a Welding Speed of 105-110 mm/min, the current setting between 80-85 A and a Gas Flow Rate of 14.5-15 l/min.
- Fractography analysis indicated that dimples and tear ridges on the fractured surface have been observed which shows ductility and high tensile strength. The voids and cracks with a brittle microstructure of fractured surface featured high hardness and low joint strength. The mathematical models developed provided accurate predictions.
- This study serves as a valuable resource for industry professionals aiming to create superior hybrid products through the combination of Aluminium and Stainless Steel. Furthermore, it presents a cost-effective strategy for welded product manufacturing, minimizing the need for extensive experimentation. In this study, our approach offers a valuable resource for industry professionals seeking to produce high-quality hybrid products by combining Aluminium and Stainless Steel. The cost-effectiveness of our method lies in its ability to minimize the need for extensive experimentation in the welding process. By systematically optimizing the TIG welding parameters—specifically, the Welding Current, Welding Speed, and Gas Flow Rate—through the application of Response Surface Methodology (RSM) and a Box-Behnken design, we identified optimal conditions for achieving superior results in terms of Ultimate Tensile Strength (UTS) and Micro-hardness.
- Traditional trial-and-error methods in welding processes can be time-consuming and resource-intensive. Our systematic and statistically driven approach allows industry professionals to efficiently pinpoint the ideal welding conditions without the need for exhaustive experimentation. This not only saves time but also reduces material wastage and associated costs. By understanding the precise combination of welding parameters that yield optimal results, manufacturers can streamline their production processes, leading to cost-effective and efficient manufacturing of welded products.

5. Recommendations

The following suggestions could serve as a basis for future investigations into the welding of Aluminium 6061 and Stainless Steel 304:

- The composition of the ER-Cu filler rod can be varied by adjusting the chemical composition of elements to achieve successful joining and gain higher strength of Aluminium and Stainless-Steel joint.
- Exploring the influence of thermal tensioning on residual stress and distortion could be an area of further investigation.

- Finite Element Simulation can also be performed to validate the results of Residual Stresses and Distortion.
- Moreover, the application of other statistical methodologies like Taguchi, Genetic Algorithm, Grey Rational Analysis, and ANN (Artificial Neural Network) may provide further insights into the analysis of results.

6. References

[1] M. Cheepu, B. Srinivas, N. Abhishek, T. Ramachandraiah, S. Karna, D. Venkateswarlu, S. Alapati, and W.S. Che, "Dissimilar joining of stainless steel and 5083 aluminum alloy sheets by gas tungsten arc welding brazing process", IOP Conference Series: Materials Science and Engineering, volume 330, page 012048. IOP Publishing, 2018.

[2] H. He, W. Chuansong, S. Lin, and C. Yang, "Pulsed tig welding– brazing of aluminum–stainless steel with an al-cu twin hot wire", Journal of Materials Engineering and Performance, 28(2):1180–1189, 2019.

[3] S. Kotari and E. Punna, "Mechanical and metallurgical investigation of tig welded-brazed aluminum and stainless steel dissimilar joint by using copper filler rod".

[4] L. Singh, R. Singh, N.K. Singh, D. Singh, and P. Singh, "An evaluation of tig welding parametric influence on tensile strength of 5083 aluminium alloy", Int. J. Mech. Aerospace, Ind. Mechatronics Eng, 7(11):1262–1265, 2013.

[5] J. Pasupathy and V. Ravisankar, "Parametric optimization of tig welding parameters using taguchi method for dissimilar joint (low carbon steel with aa1050)", Journal of Scientific and Engineering Research, 4:25–28, 2013.

[6] M. Ishak, N.F.M. Noordin, A.S.K. Razali, L.H.A. Shah, and F.R.M. Romlay "Effect of filler on weld metal structure of aa6061 aluminum alloy by tungsten inert gas welding", International Journal of Automotive and Mechanical Engineering, 11:2438, 2015.

[7] W. Chuaiphan and L. Srijaroenpramong, "Optimization of tig welding parameter in dissimilar joints of low nickel stainless steel aisi 205 and aisi 216", Journal of Manufacturing Processes, 58:163–178, 2020.

[8] A.T. Assefa, G.M.S. Ahmed, S. Alamri, A. Edacherian, M.G. Jiru, V. Pandey, and N. Hossain, "Experimental investigation and parametric optimization of the tungsten inert gas welding process parameters of dissimilar metals", Materials, 15(13):4426, 2022.

[9] G.N. Reddy and M.V. Ramana, "Optimization of process parameters in welding of dissimilar steels using robot tig welding", IOP Conference Series: Materials Science and Engineering, volume 330, page 012096. IOP Publishing, 2018.

[10] V.N. Nguyen, Q.M. Nguyen, and S.C. Huang, "Microstructure and mechanical properties of butt joints between stainless steel sus304l and aluminum alloy a6061-t6 by tig welding", Materials, 11(7):1136, 2018.

[11] H. He, S. Lin, C. Yang, C. Fan, and Z. Chen, "Combination effects of nocolok flux with ni powder on properties and microstructures of aluminum-stainless steel tig welding-brazing joint", Journal of materials engineering and performance, 22(11):3315–3323, 2013.

[12] S. Chen, J. Huang, K. Ma, X. Zhao, and A. Vivek, "Microstructures and mechanical properties of laser penetration welding joint with/without ni foil in an overlap steel-on-aluminum configuration", Metallurgical and Materials Transactions A, 45(7):3064–3073, 2014.

[13] J.L. Song, S.B. Lin, C.L. Yang, C.L. Fan, and G.C. Ma, "Analysis of intermetallic layer in dissimilar tig welding–brazing butt joint of aluminium alloy to stainless steel", Science and Technology of Welding and Joining, 15(3):213–218, 2010.

[14] G.S. Saputro, N. Muhayat, et al., "Welding current and shielding gas flow rate effect to the intermetalic layer formation of tungsten inert gas (tig) on dissimilar metals weld joints between galvanized steel and

aluminium aa 5052 by using al-si 4043 filler", Mekanika, 16(1), 2017.

[15] M.F. Benlamnouar, M. Hadji, R. Badji, N. Bensaid, T. Saadi, S. Senouci, et al., "Optimization of tig welding process parameters for x70-304l dissimilar joint using taguchi method", Solid State Phenomena, volume 297, pages 51–61. Trans Tech Publ, 2019.

[16] P. Kannan, K. Balamurugan, and K. Thirunavukkarasu, "Influence of silver interlayer in dissimilar 6061-t6 aluminum mmc and aisi 304 stainless steel friction welds", The International Journal of Advanced Manufacturing Technology, 81(9):1743– 1756, 2015.

[17] T. Xu, S. Zhou, H. Wu, C. Hong, and X. Ma, "Effect of nickel interlayer thickness on lap joint laser welding for aluminium-steel dissimilar materials", Science and Technology of Welding and Joining, 27(3):166–175, 2022.

[18] L.H. Shah, Z. Akhtar, and M. Ishak, "Investigation of aluminum-stainless steel dissimilar weld quality using different filler metals", International Journal of Automotive and Mechanical Engineering, 8, 2013.

[19] V. Chaudhari, V. Bodkhe, S. Deokate, B. Mali, and R. Mahale, "Parametric optimization of tig welding on ss 304 and ms using taguchi approach", Int. Res. J. Eng. Technol, 6(5):880–885, 2019.

[20] P. Sharma and D.K. Dwivedi, "Comparative study of activated flux-gtaw and multipass-gtaw dissimilar p92 steel-304h ass joints", Materials and Manufacturing Processes, 34(11):1195–1204, 2019.

[21] J. Kar, S.K. Roy, and G.G. Roy, "Effect of beam oscillation on microstructure and mechanical properties of aisi 316l electron beam welds", Metallurgical and materials transactions A, 48(4):1759–1770, 2017.

[22] C.Y. Cui, X.G. Cui, X.D. Ren, T.T. Liu, J.D. Hu, and Y.M. Wang, "Microstructure and Micro-hardness of fiber laser butt welded joint of stainless steel plates", Materials and Design, 49:761–765, 2013.

[23] W. Chuaiphan and L. Srijaroenpramong, "Optimization of gas tungsten arc welding parameters for the dissimilar welding between aisi 304 and aisi 201 stainless steels", Defence technology, 15(2):170–178, 2019.

[24] W. Chuaiphan and L. Srijaroenpramong, "Effect of welding speed on microstructures, mechanical properties and corrosion behavior of gta-welded aisi 201 stainless steel sheets", Journal of Materials Processing Technology, 214(2):402–408, 2014.

[25] P. Anbarasu, R. Yokeswaran, A.G. Antony, and S. Sivachandran, "Investigation of filler material influence on hardness of tig welded joints", Materials Today: Proceedings, 21:964–967, 2020.

[26] X. Yu, D. Fan, J. Huang, C. Li, and Y. Kang, "Arc assisted laser welding brazing of aluminum to steel", Metals, 9(4):397, 2019.

